

Figure 1: Cartoon of a filter membrane made up of randomly oriented fibers. Fluid flow is modeled through an imposed vertical pressure  $p_+$ , while the filter bottom is exposed to atmospheric pressure. The right figure zooms in on the fiber matrix structure assumed for the membrane, with some of the parameters indicated in the figure.

## 1 Fluid model for membrane filtration

In this sub-problem, our goal was to consider a filter consisting of randomly oriented fibers whose function is to filter out solute from a fluid flowing through it (see Figure 1, similar to the setup in [2, 3]). The motivation for answering this question lies in the fact that transport and filtration experiments are easy to carry out in the membrane before it is rolled and compressed into cannisters or cartridges. After the necessary compression step in filter manufacturing, filtration parameters are no longer known. Therefore, we set out to develop the mathematical theory and simulations that would allow prediction of transport properties of the packaged filter.

Our approach is to mathematically characterize an idealized fibrous structure, and use fiber matrix structure theory to relate transport parameters to fiber matrix properties [1–5]. Some of the parameters we model include Darcy permeability of the fluid, void fraction (i.e., void space distribution in the filter), species fraction, effective tracer diffusivity, and the retardation/sieving coefficient. A complete list of the parameters we consider is summarized in Table 1. Ultimately, we are interested in examining how changes in filter compression affect these transport and

Table 1: Fiber matrix structure parameters

Parameter	Definition
$K_{p_{eff}}$	Darcy coefficient/permeability
$\mu$	fluid viscosity
$f$	retardation/sieving coefficient
$\gamma$	partition coefficient/species volume fraction
$\epsilon$	void fraction
$r_f$	fiber radius
$r_s$	solute particle radius
$\delta$	distance between fiber bundles
$A$	surface area of the tracer
$L_u$	uncompressed membrane thickness
$L_c$	compressed membrane thickness

filtration parameters, as well as the tracer concentration time evolution.

We consider the filtration flow problem through a fiber matrix porous medium, coupled to an advection-diffusion equation for the absorption of tracer to the filter fibers (similar to the approach in [2, 3]). We therefore consider Darcy's law relating the fluid velocity to pressure:

$$\mathbf{u} = \frac{-K_{p_{eff}}}{\mu} \nabla p, \quad (1)$$

where  $\mathbf{u}$  is the fluid velocity, and  $p$  is the fluid pressure.

The continuity equation

$$\nabla \cdot \mathbf{u} = 0 \quad (2)$$

then yields

$$\nabla \cdot \left( \frac{-K_{p_{eff}}}{\mu} \nabla p \right) = 0. \quad (3)$$

The advection-diffusion equation for the concentration of tracer is given by:

$$\frac{\partial c}{\partial t} + \frac{1}{\gamma} \nabla \cdot (f c \mathbf{u}) = D_{eff} \nabla^2 c, \quad (4)$$

where  $c$  is the concentration of solute inside filter.

We thus consider the system composed of equations (3) - (4) for our model of fluid filtration through a porous medium membrane. We note that all the parameters in this equation (with the exception of viscosity  $\mu$ ) are dependent on the value of  $\epsilon$  (void fraction) of the material

considered [1–4]. The expressions for the model parameters are given by:

$$D_{\text{free}} = \frac{kT}{6\pi\mu r_s}, \quad (5)$$

$$D_{\text{eff}} = D_{\text{free}} e^{-\sqrt{1-\epsilon}\left(1+\frac{r_s}{r_f}\right)}, \quad (6)$$

$$\psi = e^{-\sqrt{1-\epsilon}\left(\frac{2r_s}{r_f} + \frac{r_s^2}{r_f^2}\right)}, \quad (7)$$

$$f = 1 - (1 - \psi)^2, \quad (8)$$

$$K_p = \frac{r_f^2 \epsilon^2}{4G(1 - \epsilon^2)}, \quad (9)$$

$$G = \frac{2}{3} \frac{2\epsilon^3}{(1 - \epsilon) \left( \ln\left(\frac{1}{(1-\epsilon)}\right) - \frac{1}{(1+(1-\epsilon)^2)} \right)} + \frac{1}{3} \frac{2\epsilon^3}{(1 - \epsilon) \left( 2 \ln\left(\frac{1}{(1-\epsilon)}\right) - 3 + 4(1 - \epsilon) - (1 - \epsilon)^2 \right)}, \quad (10)$$

$$\epsilon = 1 - \frac{3r_f^2}{\delta^2}, . \quad (11)$$

We also note that the coupling of the equations occurs through the velocity term  $\mathbf{u}$  in equation (4).

In terms of boundary conditions, we consider the following for pressure:

$$p(z = 0) = p_+ \quad (12)$$

$$p(z = L) = p_-, \quad (13)$$

where  $p_+$  corresponds to the applied pressure of the fluid, and  $p_-$  corresponds to the atmospheric pressure (see Figure 1). For the concentration of solute, we impose the following boundary conditions:

$$c(z = 0) = c_+ \quad (14)$$

$$c_z(z = L) = 0, \quad (15)$$

so that the concentration starts at level  $c_+$  at the inlet boundary, and there is no flux of solute downstream of the filter.

### 1.1 Uncompressed case for uniform void fraction $\epsilon$

We begin by considering uniform void fraction  $\epsilon$ , so that it does not depend on concentration. This means that equation (3) for pressure is uncoupled from the system. We also consider the problem in 1D, which reduces the system to:

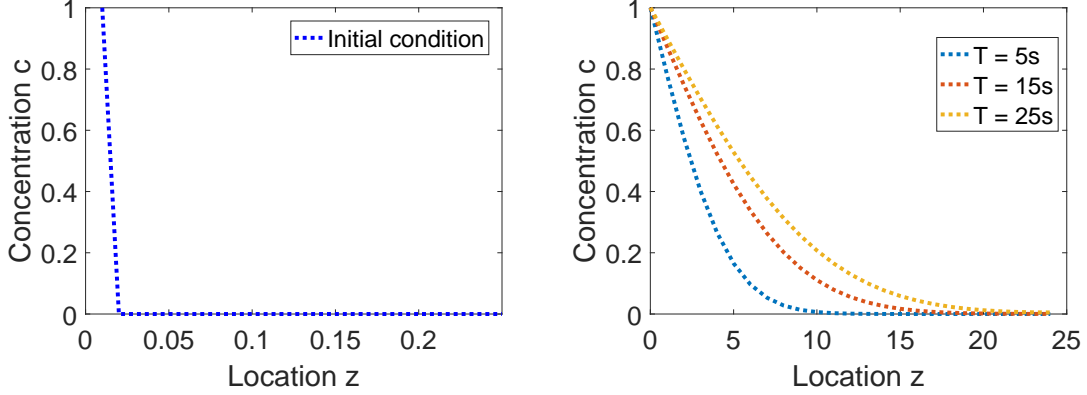


Figure 2: Left: initial condition for the concentration in the uncompressed membrane case. Right: evolution of the concentration profile for  $T = 5\text{s}$ ,  $T = 15\text{s}$ , and  $T = 25\text{s}$ .

$$p_{zz} = 0, \\ c_t + \frac{f}{\gamma} c_z u = D_{eff} c_{zz}.$$

Non-dimensionalization further yields:

$$p_{zz} = 0, \\ c_t + \tilde{b} c_z p_z = Pe^{-1} c_{zz}, \quad (16)$$

with  $\tilde{b} = \frac{f K_p}{\gamma \mu}$ , and  $Pe$  is the Peclet number:  $Pe = \frac{K_p P}{\mu D_{free}}$ , where  $P = 10 \text{ psi} \approx 68948 \text{ Pa}$  is the pressure scale considered.

The system (16) with boundary conditions (12), (14) is discretized spatially and a Crank-Nicholson time integration scheme is implemented. To account for the nonlinearity in the concentration equation, we set up the system as a Newton's iteration scheme whose solution constitutes the variables at the next time point. Simulations of the system with relevant parameters for the Gore filter membranes are illustrated in Figure 2. We take the concentration initial condition as a piecewise function in the left panel of Figure 2, and assume that the pressure decreases linearly in space from  $p_+$  to  $p_-$ . The right panel of Figure 2 shows the evolution of the concentration profile as time increases. We note that the concentration increases down the membrane, since the model (16) does not account for clogging at the top of the membrane. We also note that the pressure does not change with time, since the pressure simply satisfies the second order equation  $p_{zz} = 0$ .

## 1.2 Compressed case for uniform void fraction $\epsilon$

We assume a linear model for the effect of membrane compression on the void fraction  $\epsilon$ . Assuming that  $L_u$  is the uncompressed membrane length and  $L_c$  is the length after compression, we have the following equality by conservation of solid mass:

$$AL_u(1 - \epsilon_u) = AL_c(1 - \epsilon_c), \quad (17)$$

where the left side corresponds to the volume of solid in the uncompressed case, and the right side corresponds to the solid volume in the compressed case. Given  $\epsilon_u$  from pre-compression experiments, we can therefore choose  $\epsilon_c$  satisfying:

$$\frac{1 - \epsilon_u}{1 - \epsilon_c} = \frac{L_c}{L_u}.$$

The results given various compression ratios  $\frac{L_c}{L_u}$  are summarized in Figure 3. The differences between the uncompressed and compressed scenarios on the concentration profiles are more pronounced for smaller compression ratios, i.e., more compression of the filter membrane (right column). As mentioned in the previous section, the increase of the concentration down the membrane is due to the absence of clogging in the model.

## 2 Mechanical model

Based on the the microstructure of the membrane made of PTFE(possibly), as shown in figure 4, it is possible that the mechanical property of the membrane is highly depend on the fiber length between nodes, based on the microstructure of the membrane, there are several choices of assumptions we can make in order to simplify the problem:

- fibers (between each nodes) do not bend or buckle but the angles between fibers attached on the same node could change.
- fiber bend and buckle but angles remain the same.
- fiber bend, buckle and the angles could change.

Among the three choices of assumptions, we first discuss the first case which the fibers do not bend or buckle but can be compressed and stretched. We used a method called the stiffness method.

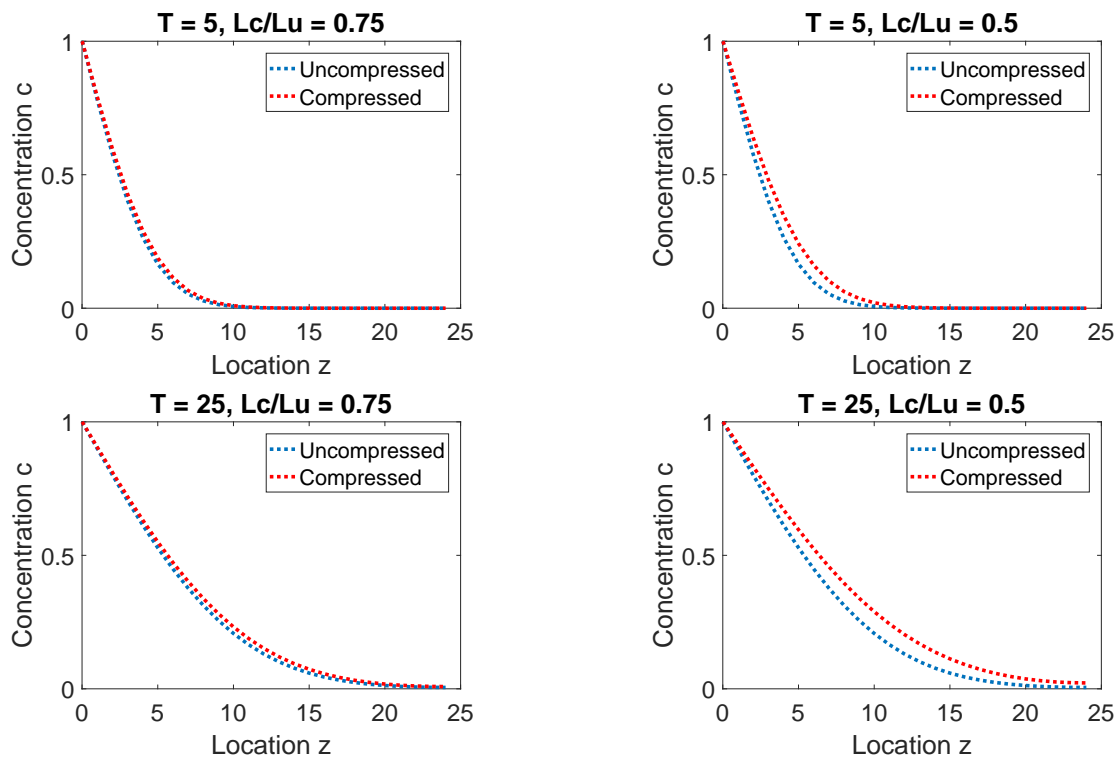


Figure 3: Fluid concentration profiles  $c$  at times  $T = 5$ s (top row) and  $T = 25$ s (bottom row). Compression ratio  $L_c/L_u = 0.75$  is shown in the left column, and  $L_c/L_u = 0.5$  in the right column.

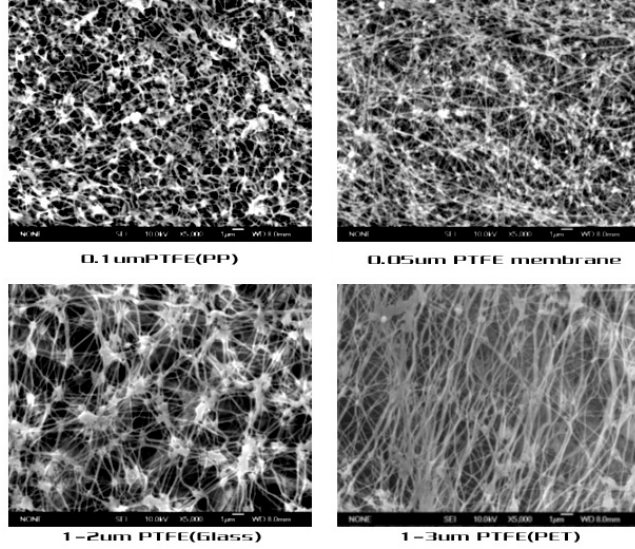


Figure 4: Different microstructures of the membrane of PTFE based on the length of the fiber. see <http://www.baghouse.com/products/baghouse-filters/ptfe-filters/>

## 2.1 Stiffness Method

In the stiffness method, we are going to construct the "stiffness matrix" of the fibrous structure such that

$$f = [K]d \quad (18)$$

where  $f$  is the vector represents the forces acting on each node in three directions ( $x, y, z$ ),  $d$  is the vector of the changes of location of each node in three directions ( $x, y, z$ ). We begin to construct  $[K]$  by following steps:

1. Divide the structure into two sets: MEMBERS(fibers or edges) and NODES(knots)
2. For each member, we consider the local relation of the axial forces ( $q_1, q_2$ ) and displacements ( $u_1, u_2$ ), and the relation can be written as

$$\mathbf{q} = k\mathbf{u} \quad (19)$$

$$\text{where } k = \begin{bmatrix} 1 & -1 \\ -1 & 1 \end{bmatrix}.$$

3. Use coordinate transformation to assign the contribution of each member's local displacement and force into the global coordinate system. For each member,

$$\mathbf{u} = T\mathbf{v} \quad (20)$$

$$\mathbf{f} = T^t \mathbf{q} \quad (21)$$

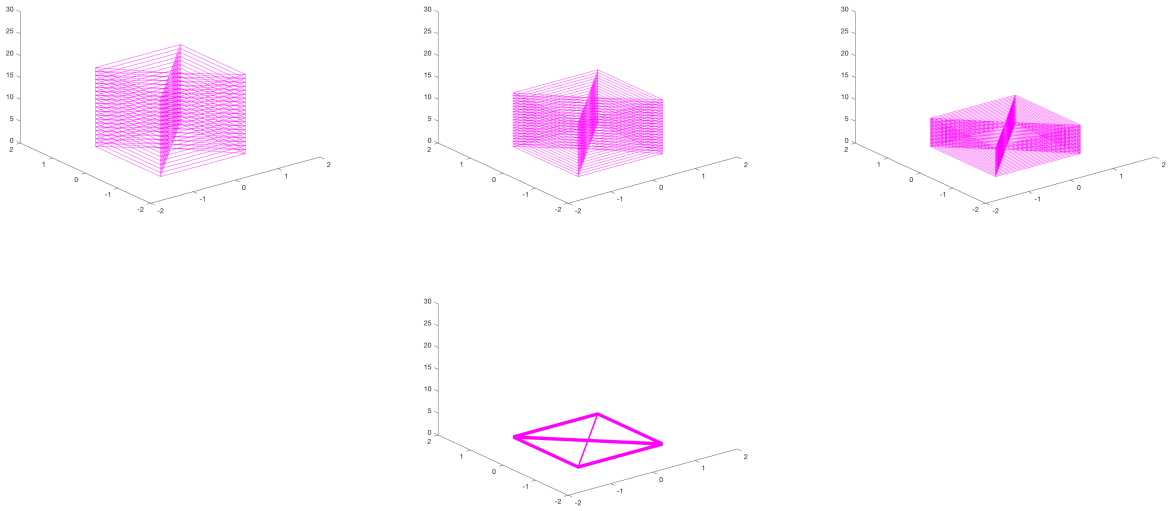


Figure 5: Simulation of compression of a stack of fibrous cube with symmetric connection, this validates our model

where  $T$  is the coordinate transformation matrix, and  $T^t$  is the transpose of  $T$ .

4. Assemble each forces and displacements of each element into one vector  $\mathbf{f}$  and  $\mathbf{v}$ .

For more detailed tutorial, see <http://people.duke.edu/~hpgavin/cee421/truss-3d.pdf>, or

<https://engineering.purdue.edu/~aprakas/CE474/CE474-Ch5-StiffnessMethod.pdf>.

In the simulation, we used the Matlab code "Truss Analysis" written by Hossein Rahami and updated by Frank McHugh. We present the following simulations by compressing a cubic fibrous "rod" and a fibrous cube.

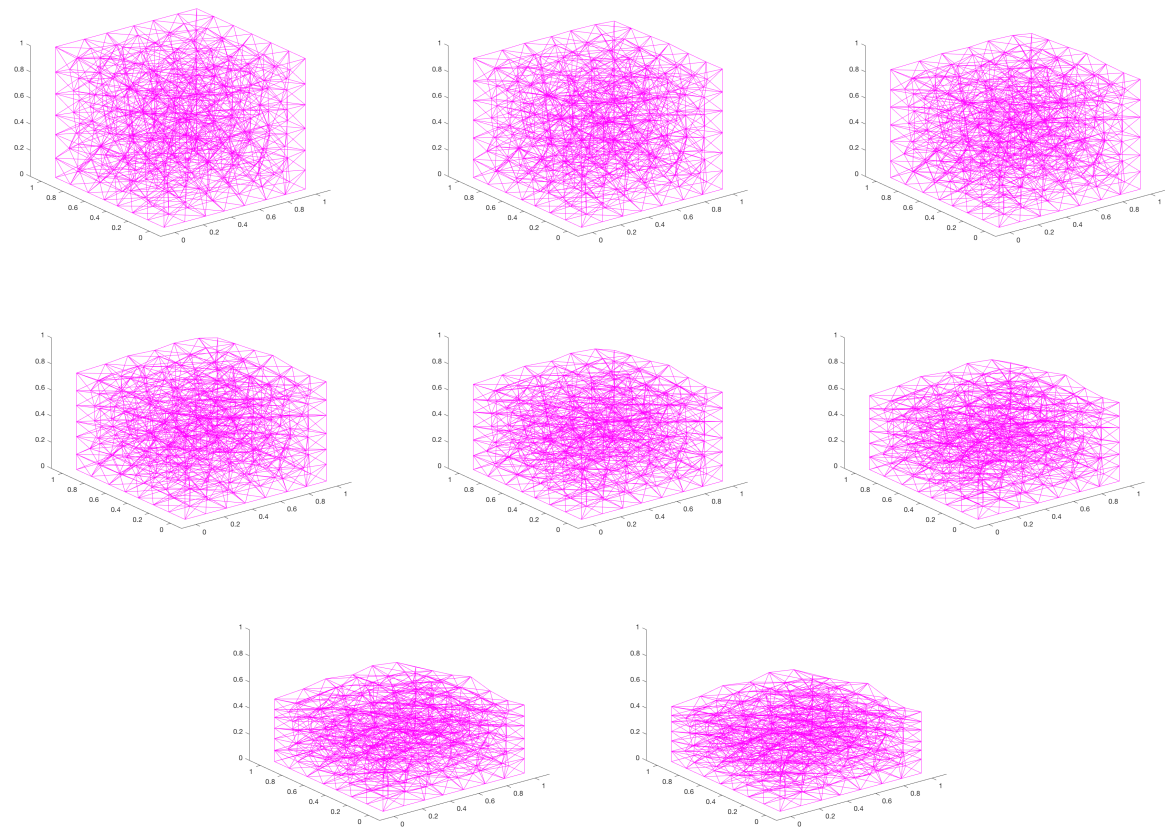


Figure 6: Simulation of compression of a fibrous cube whose fibers are extracted from the edges of a meshed cube

## 2.2 Remarks

- Random fiber orientations (or random distribution of the nodes) needs to be considered in this model rather than extracting edges from a mesh.
- Boundary conditions needs to be carefully determined, for example, in both compression cases, the nodes on the edges and four sides of the cubes only bear vertical forces, which means we are attaching wheels on all those nodes against a fixed wall.

## 3 Kirchhoff rod theory

Next we pursue a separate approach to contemplate the compression of porous membranes into filters. This is inspired by noting that a porous membrane can be made of a fibrous mesh that traps particles between the fibers. We will model the effects of compression on the shape of a single fiber, by considering a fiber to be a planar Kirchhoff rod. This places us in the context of the theory of finite displacement (via bending and twisting) of thin rods. Deformations of infinitesimal pieces of the rod may be small, but can effect a large deformation of the rod as a whole.

### 3.1 Derivation of ODE System

Consider the centerline of a rod to be a curve in the xz-plane, with position parameterized by arc length  $s$  as follows

$$\vec{r}(s) = x(s)\hat{i} + z(s)\hat{k}. \quad (22)$$

Take  $\hat{e}_1(s)$  to be the unit normal vector to the curve and  $\hat{e}_3(s)$  to be the unit tangential vector to the curve, so that

$$\hat{e}_3 = \frac{d\vec{r}}{ds} = x'(s)\hat{i} + z'(s)\hat{k}. \quad (23)$$

We must also take into account the rod curvature  $\kappa$ , which corresponds to the direction  $\hat{j}$  out of the page via the unit binormal vector  $\hat{e}_2(s)$ . Let

$$\vec{k} = \kappa\hat{j} = \kappa\hat{e}_2.$$

By definition, curvature of a smooth curve with position vector  $\vec{r}(s)$  and unit tangent vector  $\hat{e}_3(s)$  is given by

$$\kappa = \left\| \frac{d\hat{e}_3}{ds} \right\|.$$

Accordingly, we have

$$\frac{d\hat{e}_3}{ds} = \vec{k} \times \hat{e}_3, \quad (24)$$

and similarly,

$$\frac{d\hat{e}_1}{ds} = \vec{k} \times \hat{e}_1. \quad (25)$$

Then substituting for  $\vec{k}$  and  $\hat{e}_3$  in equation (24) implies

$$\begin{aligned} \frac{d\hat{e}_3}{ds} &= \kappa \hat{j} \times [x'(s)\hat{i} + z'(s)\hat{k}] \\ &= \kappa [z'(s)\hat{i} - x'(s)\hat{k}]. \end{aligned} \quad (26)$$

Now define  $\phi(s)$  to be the tangent vector's angle from the x-axis, with  $x'(s) = \cos(\phi)$  and  $z'(s) = \sin(\phi)$ , so that by substitution into equation (26),

$$\frac{d\hat{e}_3}{ds} = \kappa [\sin(\phi)\hat{i} - \cos(\phi)\hat{k}]; \quad (27)$$

and also by substitution into equation (23),

$$\hat{e}_3 = \cos(\phi)\hat{i} + \sin(\phi)\hat{k}, \quad (28)$$

which implies

$$\frac{d\hat{e}_3}{ds} = -\sin(\phi) \frac{d\phi}{ds} \hat{i} + \cos(\phi) \frac{d\phi}{ds} \hat{k}. \quad (29)$$

Equating the right hand sides of equations (27) and (29), we derive for curvature

$$\kappa = -\frac{d\phi}{ds} \quad (30)$$

Furthermore, from equations (24) and (27) we have that

$$\hat{e}_1 = \hat{e}_2 \times \hat{e}_3 = \sin(\phi)\hat{i} - \cos(\phi)\hat{k} \quad (31)$$

Keeping in mind this planar representation of a curve (the centerline of our rod), we use constitutive relationships between moments and curvature to derive an eighth-order ODE system describing the curve's deformation due to a load at its ends. This will represent a single fiber in a fibrous membrane under compression.

Let  $\vec{F}(s)$  be the force vector and  $\vec{M}(s)$  be the moment vector. Recall that the moment measures the tendency of the force to rotate the object (such as our rod) about a point or axis. Let  $E$  be Young's modulus and  $I$  be the moment of inertia of a cylinder, and recall curvature  $\kappa$ . Then for the force and the moment, respectively, we have:

$$\vec{F} = F_1(s)\hat{e}_1 + F_3(s)\hat{e}_3, \quad (32)$$

and

$$\vec{M} = EI(\kappa - \kappa''(s))\hat{e}_2. \quad (33)$$

Taking the derivative of both sides of equation (33) with respect to  $s$ , recalling  $\frac{d\hat{e}_2}{ds} = 0$ , we get

$$\vec{M}'(s) = EI \frac{d}{ds}[\kappa - \kappa'']\hat{e}_2,$$

which implies

$$\frac{M_2}{EI} = \kappa - \kappa''. \quad (34)$$

From the balance of linear and angular momentum, according to general Kirchhoff rod theory, we have relationships

$$\vec{F}''(s) = \vec{0} \quad (35)$$

and

$$\vec{M}'(s) + \hat{e}_3 \times \vec{F} = \vec{0}. \quad (36)$$

Substituting equation (32) into equation (36) implies

$$M'_2 = -F_1. \quad (37)$$

Next, taking the second derivative of equation (32) and substituting equations (24) and (25), we see that the constitutive force equation (35) implies

$$\vec{F}'' = [F''_1 - \kappa^2 F_1 + \kappa' F_3 + 2\kappa F_3] \hat{e}_1 + [F''_3 - \kappa^2 F_3 - \kappa' F_1 - 2\kappa F'_1] \hat{e}_3 = 0 \quad (38)$$

### 3.2 Kirchhoff Rod ODE System

Thus, from equations (30), (34), (37), and (38), we extract the eighth-order ODE system describing the rod's centerline:

$$\begin{aligned} \phi'(s) &= -\kappa \\ \kappa'' - \kappa &= \frac{-M_2}{EI} \\ M'_2 &= -F_1 \\ F''_1 &= \kappa^2 F_1 - \kappa' F_3 - 2\kappa F'_3 \\ F''_3 &= \kappa^2 F_3 + \kappa' F_1 + 2\kappa F'_1 \end{aligned} \quad (39)$$

We can solve this system in MATLAB, given eight boundary conditions. The conditions we

consider to start with include no shear force at the rod ends

$$F_1(0) = F_1(L) = 0, \quad (40)$$

a load at the ends (the compression force)

$$F_3(0) = -F_3(L) = -N, \quad (41)$$

constant curvature at the rod ends

$$\kappa'(0) = \kappa'(L) = 0, \quad (42)$$

no torque at the bottom, such as from fixing the rod to the base

$$M_2(0) = 0, \quad (43)$$

and the rod standing straight up at the base

$$\phi(0) = \pi/2. \quad (44)$$

## 4 Future work

### Fluid flow through filters

In the fiber matrix model described in Section 1, we considered fluid flow through a filter membrane, and prescribed boundary conditions for the pressure on the top and bottom of the membrane. A more realistic boundary condition that we plan to implement is prescribing the flow  $Q = -\frac{K_p}{\mu} Ap_z$  at the inlet boundaries rather than the pressure, as this may be more easily available from experiments. Moreover, a more realistic model for the fluid flow can be explored by introducing clogging through the equation:

$$\frac{d\xi}{dt} = kc, \quad (45)$$

where  $\xi$  corresponds to the amount of bound solute, and  $k$  is a rate parameter. This  $\xi$  is subsequently subtracted from equation (11) for void fraction  $\epsilon$ , making all other parameters also dependent on  $\xi$  (and therefore time-varying). This will yield a dynamic pressure distribution, and will fully couple equations (3) - (4).

## Mechanical fiber model

For the mechanical model presented in Section 2, we propose the following improvements:

- Random distributed fibers needs to be applied.
- Buckling of the fibers needs to be considered by adding two more components  $\phi, \theta$  on the unknown vector  $\mathbf{u}$  which denotes the angular momentum in 3D.
- Mechanical properties of the membrane should be considered for the realistic case.
- Find a way to get the filter parameters as well as the changes of the macroscopic level from the microscopic level simulation, i.e. bubble point, porosity, etc.
- A more realistic boundary condition needs to be considered. For example, if the nodes on the edges or surfaces of the cube are allowed to move horizontally, some of the nodes might be compressed "out of" the cube and the deformation of those fibers attached to the nodes are very large, which is unrealistic. Therefore buckling or even failure of such fibers shall be considered.

## References

- [1] F. CURRY, *Mechanics and thermodynamics of transcapillary exchange*, Handbook of physiology, 4 (1984), pp. 309–374.
- [2] Y. HUANG, D. RUMSCHITZKI, S. CHIEN, AND S. WEINBAUM, *A fiber matrix model for the growth of macromolecular leakage spots in the arterial intima*, Journal of biomechanical engineering, 116 (1994), pp. 430–445.
- [3] Y. HUANG, D. RUMSCHITZKI, S. CHIEN, AND S. WEINBAUM, *A fiber matrix model for the filtration through fenestral pores in a compressible arterial intima.*, The American journal of physiology, 272 (1997), pp. H2023–39.
- [4] J. LEVICK, *Flow through interstitium and other fibrous matrices*, Quarterly journal of experimental physiology, 72 (1987), pp. 409–437.
- [5] C. MICHEL, *Fluid movements through capillary walls*, Handbook of Physiology. The Cardiovascular System. Microcirculation, 4 (1984), pp. 375–409.